Fish and Shellfish Immunology 131 (2022) 160–171

Contents lists available at ScienceDirect

Fish and Shellfish Immunology

journal homepage: www.elsevier.com/locate/fsi

Full length article

Implication of adipocytes from subcutaneous adipose tissue and fatty acids in skin inflammation caused by λ-carrageenin in gilthead seabream (*Sparus aurata*)

Jose Carlos Campos-Sánchez [a], Daniel Gonzalez-Silvera [b], Xu Gong [b], Richard Broughton [b], Francisco A. Guardiola [a], Mónica B. Betancor [b], María Ángeles Esteban [a,*]

[a] *Immunobiology for Aquaculture Group, Department of Cell Biology and Histology. Faculty of Biology, Campus Regional de Excelencia Internacional "Campus Mare Nostrum", University of Murcia, 30100, Murcia, Spain*

[b] *Institute of Aquaculture, Faculty of Natural Sciences, University of Stirling, Stirling, FK9 4LA, Scotland, UK*

ARTICLE INFO

Keywords:
Carrageenin
Skin inflammation
Adipocytes
Fatty acids
Gilthead seabream *(Sparus aurata)*
Aquaculture

ABSTRACT

The role of subcutaneous adipose tissue adipocytes and the effects of fatty acids on carrageenan-induced skin inflammation in gilthead seabream (*Sparus aurata*) were studied. Fish were injected intramuscularly with phosphate-buffered saline (control) or λ-carrageenin (1%), and skin samples collected at the injection site at 3 and 6 h post-injection (p.i.) were processed for histological study. In addition, the presence and levels of lipid classes, fatty acid methyl esters (FAME) and eicosanoids were evaluated in the skin samples obtained from the injected areas. Histological results indicated an increase in adipocyte area in fish sampled at 3 h p.i. with λ-carrageenin compared to fish in the control group. Furthermore, the frequency of adipocytes between 4500 and 5000 μm^2 was increased at 6 h in the λ-carrageenin group compared to the control group. Analysis of lipid classes found that fish injected with λ-carrageenan showed increased free fatty acid (FFA) and sphingomyelin content at 3 and 6 h, respectively, compared to the control group. An increase in saturated fatty acids (SFA), n-6 polyunsaturated fatty acids (PUFA), and a decrease in the values of monounsaturated fatty acids (MUFA), n-3 PUFA and minor fatty acids were observed in fish skin at 6 h after λ-carrageenin injection, with respect to the values obtained in the control group. Regarding the analysis of eicosanoids, an increase in hydroxyeicosatetraenoic acid (5-HETE) was detected in the skin of fish at 6 h post-carrageenin injection compared to the control group. The presented results indicate the contribution of adipocytes and fatty acids in the development and regulation of the inflammatory response triggered by λ-carrageenin in gilthead seabream skin.

1. Introduction

Inflammation consists of an intricate response orchestrated by the innate immune system to protect the host against any type of external insult or harmful stimulus, with the intention of restoring physiological homeostasis [1,2]. This complex response is usually local and characterized by specific symptoms (*e.g.*, heat sensation, redness, swelling, pain and functional disorders), which resolve within minutes, hours or days (acute inflammation) [3]. However, it can persist over time and become chronic (chronic inflammation) leading to numerous associated pathological disorders [4]. Typically, a sequence of events unfolds from the onset of inflammation, with the release of proinflammatory mediators, recruitment of immune cells to the affected area, and regulation of the inflammatory response, leading to the eventual resolution of inflammation [5]. Throughout this process, not only immune cells, but also non-immune resident cells, such as endothelial cells, fibroblasts, preadipocytes (progenitor stem cells within the vascular fraction of the stroma) or of white adipose tissue (WAT) adipocytes that often surround connective tissue and muscle, can assume a key direct role [6,7]. Among these, adipocytes are emerging as a critical niche of cells within multiple tissues capable of responding to external stimuli by changing their morphology and function (WAT remodelling), as well as secreting hormones, adipokines (*e.g.,* leptin, adiponectin and resistin) and proinflammatory cytokines [*e.g.*, interleukin-1β (IL-1β), tumor necrosis

* Corresponding author. Department of Cell Biology and Histology. Faculty of Biology, Campus Regional de Excelencia Internacional "Campus Mare Nostrum", University of Murcia, 30100, Murcia, Spain.
E-mail address: aesteban@um.es (M.Á. Esteban).

https://doi.org/10.1016/j.fsi.2022.09.066
Received 22 July 2022; Received in revised form 25 September 2022; Accepted 28 September 2022
Available online 7 October 2022

factor-α (TNF-α) and interleukin-6 (IL-6)]. These molecules regulate macrophage infiltration into the adipose tissue (AT) and thus mediate the interaction with immune cells [8–10].

Regarding adipocyte lipid metabolism, they can also activate lipolysis, hydrolysing stored triglycerides into free fatty acids (FFAs) and glycerol to support surrounding cells and tissues [11,12]. In this regard, FAs can promote inflammation through various mechanisms, such as binding to membrane surfaces or intracellular "fatty acid receptors" that can modify membrane fluidity, lipid raft formation and cell signalling, activating transcription factors involved in the inflammatory response, such as NF-κB (nuclear factor kappa-light-chain-enhancer of activated B cells) or PPAR-γ (peroxisome proliferator activated receptor-γ) [13], as well as being the precursor of pro- and anti-inflammatory eicosanoids. Moreover, the length of the FA chain and the absence of double bonds (saturated FA) or the presence (unsaturated FA) at one (monounsaturated FA; MUFA) or more positions (polyunsaturated FA; PUFA) of the acyl chain appear to be critical in their function [13]. Polyunsaturated fatty acids with C $\geq$ 20 are referred to as long chain PUFA (LC-PUFA) and, depending on the location of the last double bond, PUFAs can be classified as n-3 and n-6 [14]. Once absorbed, the dominant fates of dietary LC-PUFAs are incorporated into cell membrane phospholipids, neutral lipids, or metabolic oxidation. Phospholipids serve to maintain cell membrane fluidity and are stored as strategic precursors of signalling molecules in multiple inflammatory and immune pathways. Indeed, following phospholipase A2 cleavage of membrane phospholipids, cyclooxygenases (COX), lipoxygenases (LOX) and cytochrome P450 (CYTP) act to produce pro- or anti-inflammatory mediators that can be produced from n-3 and n-6 LC-PUFA. In this regard, eicosanoids, a key inflammatory mediator, can be derived from several fatty acids, such as arachidonic acid (AA, 20:4n-6) or eicosapentaenoic acid (EPA, 20:5n-3) [13,15–17]. Thus, although FAs generally appear to play a key role in inflammation, the predisposition of an organ, and its associated fatty acid complement, and response to a specific immune insult have not been extensively studied in fish.

To expand our knowledge about the mechanism and role of FAs in fish inflammation, we used carrageenin as a trigger of inflammation. Carrageenin is a sulphated mucopolysaccharide obtained from the cell walls of red algae (Rhodophyceae family) whose high-molecular weight and compound structure of α(1, 3) - β(1, 4) - galactans with one (κ-), two (ι-) or three (λ-) sulphates per disaccharide unit, confer its unique properties [18]. In particular, the degree of sulphation appears to play a key role in triggering murine inflammation, with λ-carrageenin being the main form used for this purpose [18–24]. Carrageenan has also been used in agriculture and in the pharmaceutical industry due to its antioxidant, antiviral, anticoagulant, antithrombotic, immunomodulatory and antitumor effects derived from the large negative charges it possesses, due to the sulphate groups [18]. In fact, these negative charges also allow carrageenan to form biopolymers that are being exploited in nanotechnology [25]. However, about 80% of all carrageenan produced (mostly from aquaculture algae of the genera *Chondrus, Eucheuma, Gigartina, Iridaea, Furcellaria and Hypnea* spp.) is destined for culinary uses, being used as additives (E 407, E 407a), emulsifiers or stabilizers in many foods due to its thickening and suspension characteristics [26–28]. However, it is important to note that carrageenan is not assimilated by the human body due to its strange structure, acting as a fiber with no nutritional value [28]. In fish, carrageenin has been used to induce inflammation at different body sites in several fish species, such as plaice (*Pleuronectes platessa*) [29], carp (*Cyprinus carpio*) [23], Nile tilapia (*Oreochromis niloticus*) [30], pacu (*Piaractus mesopotamicus*) [31,32] and zebrafish (*Danio rerio*) [33–35]. More recently, the inflammatory response of gilthead seabream (*Sparus aurata*) has been studied by our team, providing diverse information on gene expression [36,37], humoral and cellular immune parameters [38] and the use of non-invasive techniques such as real-time ultrasound or micro-CT to study this complex process [39]. In addition, previous work has evidenced the local effect of mucus-secreting cells of the skin in the inflamed area at 3 h after carrageenin injection by immunohistochemical assay [40]. All these previous results encouraged us to perform the present study, looking for the possible role of other non-immune resident cells in the area of inflammation. With these considerations in mind, the present trial aimed to evaluate the role of subcutaneous adipose tissue (SAT) adipocytes and changes in the lipid profile in gilthead seabream skin after provoking an acute experimental inflammation by intramuscular injection of λ-carrageenin.

2. Material and methods

2.1. Animals

Twenty-eight specimens (20.87 ± 5.6 g mean weight) of the seawater teleost gilthead seabream, obtained from a local farm (Mazarrón, Spain), were maintained in marine re-circulating aquaria (450 L) at the Marine Fish Facilities of the University of Murcia (Spain) during a quarantine period of one month. Water temperature was maintained at 20 ± 2 °C with a flow rate of 900 L h^{-1}, a salinity of 28‰, a photoperiod of 12 h light to 12 h dark and continuous aeration. Fish were fed a commercial diet (Skretting, Spain) at a rate of 2% body weight day^{-1} and were kept 24 h without feeding prior to the trial. All experimental protocols were approved by the Ethical Committee of the University of Murcia (A13160416), and the Animal Welfare and Ethical Review Board at the University of Stirling (AWERB/2022/8491/6802). All procedures were performed following the Guidelines of the European Union (2010/63/EU) and Spanish Legislation (RD 1201/2005 and Law 32/2007) for the use of laboratory animals.

2.2. Experimental design and sample collection

Fish were randomly selected, anesthetized with clove oil (20 mg L^{-1}, Guinama®), and injected intramuscularly in the left flank, below the lateral line at the level of the second dorsal fin. Two groups of fish were established: *i)* fish injected with 50 μL of phosphate-saline buffer (PBS, control group); and *ii)* fish injected with 50 μL of λ-carrageenin (1% in PBS, Sigma-Aldrich). Each experimental group was composed of 14 fish, placed into two tanks (two replicates, 7 fish per tank) of 250 L, rate flow of 800 L h^{-1} and continuously aerated. At 3 and 6 h post-injection, seven fish from each tank were weighed and samples of the skin were collected from the injected area with an 8 mm diameter metal biopsy punch (Stiefel). The fish were then returned to the same tank. Immediately, skin biopsies from each fish were divided into three parts: *i)* one part was washed in PBS and processed for histological analysis, *ii)* another part was freeze-dried (CHRIST, Model Alpha 1–2 LD, 101,021) and stored in the dark at −20 °C, *iii)* the last part was stored in TRIzol® (Invitrogen) at −80 °C for gene expression analysis.

2.3. Histological study

For histological study, the skin samples were fixed in 10% neutral buffered formalin (Panreac, Spain) at room temperature for 24 h. Subsequently, the samples were decalcified in a solution of methylenediaminetetraacetic acid (EDTA, Sigma-Aldrich) 0.5 M for 24 h. The samples were then dehydrated in increasing concentrations of ethanol (Merck) (50% for 30 min, 70% for 24 h, 80% for 30 min, 96% for 1 h, and 100% for 1 h three times), washed for 1 h three times in isoamyl acetate, and finally embedded in Histoplast Paraffin (Thermo Fisher Scientific). Each paraffin block was cut into serial sections (4 μm thick) using a microtome (Leica RM2265), mounted on sialinate-coated slides (Dako, Glostrup, Denmark) and stored at room temperature. Sections were stained with hematoxylin-eosin (H&E, Bio-Optica), according to the manufacturer's instructions, and the slides were scanned using the Leica SCN400F Brightfield and fluorescence scanner (Leica, Microsystems). Quantitative histomorphometric evaluation was performed according to Parlee et al. [41] with some modifications. Open-source

software for digital pathology image analysis - QuPath-0.3.0 was used to acquire 5 representative images of each individual slide, which were analysed with ImageJ 1.49v software [42]. The area of adipocytes was expressed as μm^2, while the number of adipocytes counted was subsequently used to convert the frequency into a percentage of total adipocytes in intervals of 500 μm^2, and the values were used for statistical analysis.

2.4. Lipid analysis

Freeze-dried skin samples were processed at the Nutrition Analytical Service of the Institute of Aquaculture (University of Stirling, Scotland). The samples were weighed and divided into two parts: *i*) half was processed according to the method described by Folch et al. [43] for total lipid extraction. Briefly, samples of 10 mg were homogenized in 1 mL of chloroform/methanol (2:1 v/v) with an Ultra Turrax tissue disrupter (IKA ULTRA-TURRAX T 25 digital, IKA-WERKE). Non-lipid impurities were removed by washing with 0.88% (w/v) KCl. The lipid weight was determined gravimetrically after evaporation of the solvent and drying under vacuum overnight. Then, due to the limited amount of sample, lipids were adjusted to 2 mg mL^{-1}. *ii*) the other half of the skin sample was processed for the extraction and analysis of eicosanoids.

2.4.1. Analysis of lipid classes in skin samples

The lipid classes of the skin samples were analysed by separating them by high performance thin layer chromatography (HPTLC). Briefly, 7.5 μL of total lipid extract (2 mg mL^{-1}) was loaded in a 2 mm line on a 10 × 10 cm prewashed silica gel plate (VWR, Lutterwirth, England) by running the solvent, consisting of methyl acetate: isopropanol: chloroform: methanol: KCl 0.25% (25:25:25:10:9 in vol.), to 2/3rds of the length of the plate. After desiccation, the plate was then run with isohexane: diethyl ether: acetic acid (8:2:0.1 in vol.). The plates were sprayed with 3% (w/v) aqueous copper acetate containing 8% (v/v) phosphoric acid, and the different classes of lipids were quantified by baking the plate at 160 °C for 17 min, followed by calibrated densitometry using a TLC scanner with CAMAG "WinCATS" Planar Chromatography Manager software, version 1.2.0. Lipid classes were identified by comparison with known standards. In total, fifteen lipid classes were quantified: lysophosphatidylcholine (LPC), sphingomyelin (SM), phosphatidyl choline (PC), phosphatidyl serine (PS), phosphatidyl inositol (PI), the sum of phosphatidic acid + phosphatidyl glycerol + cardiolipin (PA/PG/CL), phosphatidyl ethanolamine (PE), unknown polar (UP), pigment (Pig) (all of them polar lipids), diacylglycerol (DAG), cholesterol/sterols (CHOL), free fatty acids (FFA), Unknown neutral (UN), triglycerides (TAG) and wax/sterol esters (WAX) (all of them neutral lipids).

2.4.2. Fatty acid methyl ester analysis

Fatty acid methyl esters (FAMEs) were prepared by acid-catalysed transesterification of total lipids according to the method of Christie [44]. Thus, total lipid samples (2 mg mL^{-1}) were transmethylated overnight in 2 mL of 1% sulphuric acid in methanol (plus 1 mL of toluene to dissolve neutral lipids) at 50 °C. Methyl esters were extracted twice in 5 mL hexane-diethyl ether (1:1, v/v) after neutralization with 2 mL 2% $KHCO_3$, dried under nitrogen and redissolved in 0.5 mL iso-hexane. The FAMEs were separated and quantified by gas-liquid chromatography using an SPTM 2560 flexible fused silica capillary column (100 m long, 0.25 mm internal diameter, 0.20 mm film thickness, SUPELCO) in a Hewlett-Packard 5890 gas chromatograph. The oven temperature of the gas chromatograph was programmed for 5 min at an initial temperature of 140 °C, increased at a rate of 4 °C min^{-1} to 230 °C, further increased at a rate of 1 °C min^{-1} to 240 °C and then held at that temperature for 6 min. The injector and flame ionization detector were set at 260 °C. Helium was used as the carrier gas at a pressure of 300 kPa, and peaks were identified by comparing their retention times with appropriate FAME standards (Sigma Chemical Company). The concentrations of individual fatty acids were expressed as percentages of the total content.

2.4.3. Eicosanoid analysis

For eicosanoid analysis, skin samples were weighed into 2 mL polypropylene tubes, followed by the addition of 10 μL of antioxidant solution [containing 0.2 mg mL^{-1} BHT and 0.2 mg mL^{-1} EDTA in methanol/water (50:50 v/v)]. Six levels of calibrant were prepared in polypropylene tubes with an additional blank (without calibrant), each tube containing 10 μL of each calibrant. 10 μL of internal standard solution (1.5 pmol μL^{-1}; Cambridge Bioscience) were added to both samples and calibrants. The samples were then mixed with 500 μL of cold methanol, homogenized using steel beads in a Minibeadbeater tissue homogeniser (3500 rpm, 2 min, Biospec Products) and mixed with another 500 μL of methanol. After 15 min incubation on ice, the samples were centrifuged (20,000×*g*, 10 min, 4 °C) and the supernatant was transferred to clean Eppendorf tubes and dried under nitrogen. Samples were resuspended in 800 μL of water/methanol (90:10 v/v), and acidified with 32 μL pure acetic acid before loading the samples onto preconditioned SPE SepPak tC18columns (Waters). The columns were first conditioned with 2 column volumes of methanol, followed by two column volumes of water. Samples were then loaded onto the columns, which were quickly washed with 2 column volumes of water, followed by 2 column volumes of hexane. The eicosanoids were eluted with 1 mL of methyl formate and transferred to new Eppendorf tubes. Samples were dried under nitrogen and resuspended in 40 μL of water:methanol (v/v) solution. To sediment the particles, the samples were centrifuged (13,000×*g*, 2 min), transferred to glass vials with low volume extraction points and 15 μL of sample was injected into the column. Analysis of skin samples was performed on a Waters Xevo TQ-S, using a Waters Class I UPLC system with an Acquity BEH C18 column (2.1 × 100 mm). The UPLC solvents (Rathburn chemicals) were composed of solvent A, containing water/acetonitrile (80:20 v/v) and formic acid (0.02% v/v), and solvent B, containing acetonitrile/isopropyl alcohol (50:50 v/v). The UPLC gradient used was 100% A for 0.5 min, then 55% solvent B for 7 min, then 100% solvent B for 3 min, which was held for 4 min. The gradient was returned to 100% solvent A for 3 min and conditioned for another 2 min. The TQ-S was run in negative mode, with a capillary voltage of –3kV, desolvation temperature of 300 °C, a desolvation gas flow rate of 800 L h^{-1} and a cone gas flow rate of 150 L h^{-1}. The system was run in MRM mode and the transitions detailed are indicated in Table 1.

2.5. Gene expression analysis by real-time qPCR

The sequences of the selected genes were obtained from a gilthead seabream database [45]. The Open Reading Frames (ORF) were located using the ExPASy translation software (SIB Bioinformatics Resource Portal) and an additional check was performed using NCBI BLAST sequence alignment analysis (NIH). Primers used (Table 2) were designed with the Thermo Fisher OligoPerfect™ tool. Total RNA was extracted from samples of 0.5 g of gilthead seabream skin using TRIzol Reagent [46], following the manufacturer's instructions and quantification and purification were assessed using a Nanodrop® spectrophotometer; the 260:280 ratios were 1.8–2.0. Then, the RNA was treated with DNase I (Promega) to remove genomic DNA contamination, and complementary DNA (cDNA) was synthesized from 1 μg of RNA using the reverse transcriptase enzyme SuperScriptIV (Life Technologies) with an oligo-dT_{18} primer. The expression of the selected genes was analysed by real-time qPCR with QuantStudio™ Real-Time PCR System Fast (Life Technologies). The reaction mixtures [containing 5 μL of SYBR Green supermix, 2.5 μL of primers (0.6 μM each) and 2.5 μL of cDNA template] were incubated for 10 min at 95 °C, followed by 40 cycles of 15 s at 95 °C, 1 min at 60 °C, and finally 15 s at 95 °C, 1 min at 60 °C and 15 s at 95 °C. The gene expression was analysed using the $2^{-\Delta Ct}$ method [47], which was performed as described elsewhere [48]. The specificity of the reactions was analysed using samples without cDNA as negative

Table 1
Adjustments of the Ultra Performance Liquid Chromatography system.

Eicosanoid name	Abbreviation	Transition	DP (V)	CE (V)	Dwell (s)
Internal quantification calibrant d4 13-Hydroxyoctadecadienoic acid	d4 13-HODE	299.2 > 198.0	60	23	0.01
Internal quantification calibrant d5 15-Hydroxyeicosapentaenoic acid	d5 15-HEPE	322.2 > 221.0	40	18	0.01
Internal quantification calibrant d8 5-Hydroxyeicosatetraenoic acid	d8 5-HETE	327.2 > 116.0	40	20	0.01
Internal quantification calibrant d5 17-Hydroxydocosahexaenoic acid	d5 17-HDHA	348.2 > 232.0	20	19	0.01
Internal quantification calibrant d4 Prostaglandin D2	d4 PGD2	355.2 > 275.0	50	23	0.01
Internal quantification calibrant d4 Thromboxane B2	d4 TxB2	373.2 > 173.0	50	22	0.01
12-Hydroxyheptadecatrienoic acid	12-HHTrE	279.2 > 217.0	30	21	0.01
13-Hydroxyoctadecatrienoic acid	13-HOTrE	293.2 > 195.0	40	28	0.01
9-Hydroxyoctadecadienoic acid	9-HODE	295.2 > 171.0	60	23	0.01
13-Hydroxyoctadecadienoic acid	13-HODE	295.2 > 195.0	60	23	0.01
5-Hydroxyeicosapentaenoic acid	5-HEPE	317.2 > 115.0	30	22	0.01
12-Hydroxyeicosapentaenoic acid	12-HEPE	317.2 > 179.0	30	19	0.01
15-Hydroxyeicosapentaenoic acid	15-HEPE	317.2 > 219.0	40	18	0.01
5-Hydroxyeicosatetraenoic acid	5-HETE	319.2 > 115.0	40	20	0.01
12-Hydroxyeicosatetraenoic acid	12-HETE	319.2 > 135.0	50	19	0.01
15-Hydroxyeicosatetraenoic acid	15-HETE	319.2 > 175.0	40	19	0.01
15-Hydroxyeicosatrienoic acid	15-HETrE	321.2 > 221.0	30	21	0.01
5,15-Dihydroxyeicosa-6,8,11,13-tetraenoic acid	5,15-diHETE	335.2 > 201.0	40	26	0.01
17-Hydroperoxydocosahexaenoic acid	17-HpDHA	341.3 > 111.2	30	12	0.01
14-Hydroxydocosahexaenoic acid	14-HDHA	343.2 > 205.0	30	18	0.01
17-Hydroxydocosahexaenoic acid	17-HDHA	343.2 > 229.0	20	19	0.01
Prostaglandin D2	PGD2	351.2 > 271.0	40	23	0.01
Prostaglandin E2	PGE2	351.2 > 271.0	40	23	0.01
Thromboxane B2	TxB2	369.2 > 169.0	50	22	0.01
6-keto-prostaglandin F1 alpha	6-Keto PGF1a	369.2 > 245.0	60	34	0.01
prostaglandin F2 alpha	PGF2a	353.2 > 193.0	50	25	0.01

Table 2
Primers used for real-time qPCR.

Gene name	Gene abbreviation	GenBank number	Primer sequences (5'→3')
Interleukin 1	*il1b*	XM030416076.1	F: GCGAGCAGAGGCACTTAGTC R: GGTAGGTCGCCATGTTCAGT
Tumor necrosis factor alpha	*tnfa*	AJ413189	F: CTGTGGAGGGAAGAATCGAG R: TCCACTCCACCTGGTCTTTC
Interleukin-6	*il6*	AM749958	F: AGGCAGGAGTTTGAAGCTGA R: ATGCTGAAGTTGGTGGAAGG
Leptin A	*lepa*	MG570179	F: GCTCCACTGGGCTTTCAAGT R: AGGTCGTCTGAGATCAGGCT
Leptin B	*lepb*	Spau1B017168	F: CACTTCTGGACCAGGAGCTG R: ACGGGACAGTTCATCGTGAC
Peroxisome proliferator activated receptor gamma	*pparg*	115583930	F: AGATAACGCGCCCTTTGTCA R: TGTTTGTGGTTGGTGCTCCT
Ribosomal protein S18	rps18	AM490061	F: CGAAAGCATTTGCCAAGAAT R: AGTTGGCACCGTTTATGGTC
Elongation factor-1 alfa	ef1a	AF184170	F: TGTCATCAAGGCTGTTGAGC R: GCACACTTCTTGTTGCTGGA
Actin beta	actb	X89920	F: GGCACCACACCTTCTACAAATG R: GTGGTGGTGAAGCTGTAGCC

controls. For each mRNA sample, gene expression was normalized with the geometric mean of ribosomal protein (*s18*), elongation factor 1-alfa (*ef1α*) and beta-actin (*actb*) RNA content. Gene names follow the accepted nomenclature for zebrafish (http://zfin.org/). In all cases, each PCR was performed on triplicate samples.

2.6. Statistical analysis

Results were expressed as mean ± standard error of the mean (SEM). The data were analysed using a two-way-ANOVA to establish significant differences between two factors: experimental group and time, and to determine the interaction of both factors. Student's t-test was used to determine the differences between experimental groups and each experimental group with respect to time. The normality of the data was previously evaluated using the Shapiro-Wilk test and the homogeneity of variance was also verified using Levene's test. Percentage data were arcsine transformed when necessary, according to the normality test, prior to statistical analysis. All statistical analyses were performed with the SPSS software package (version 25.0; SPSS) for Windows. The significance level used was $p < 0.05$ for all statistical tests.

3. Results

3.1. Skin histology

In this work our interest was focused on the possible changes observed in the subepidermal fat due to carrageenin injection. The results obtained by studying histological sections of gilthead seabream skin showed some alterations in some of the layers. The fat layer, formed by adipocytes, was easily visible in H&E-stained cross-sections of the skin and is part of the last layer of the dermis, just before the underlying muscle (Fig. 1). Adipocytes appear as large cells with a small nucleus located at the periphery of the cell and a sparse halo of cytoplasm. They are large cells with a rounded or polygonal shape, which appear white due to the space occupied by their large lipid vacuole, the contents of which were removed by the reagents used during the Paraplast

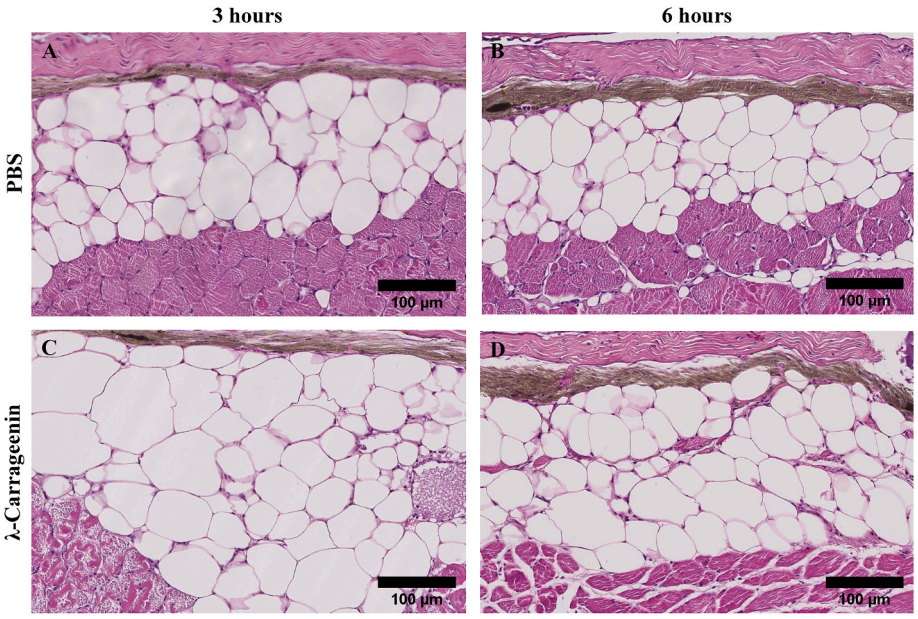

Fig. 1. Representative images of gilthead seabream subcutaneous adipose tissue at 3 and 6 h post-injection with PBS (control, A, B) or λ-carrageenin (1%, C, D) stained with hematoxylin-eosin (H–E). Adipocytes appear as large, rounded, white cells. Scale bar = 100 μm.

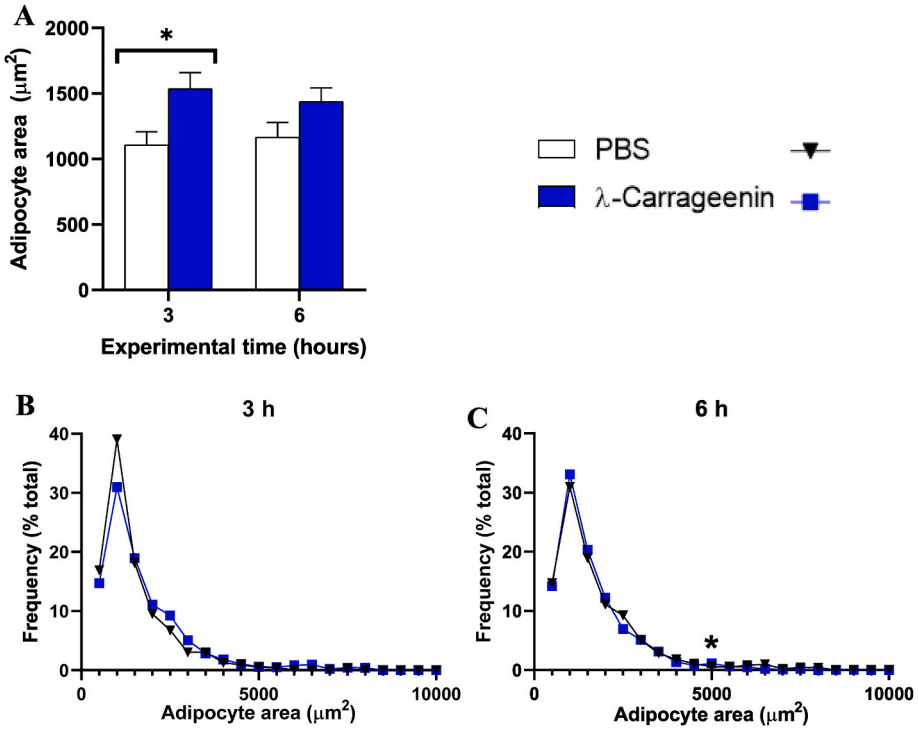

Fig. 2. Quantitative analysis of subcutaneous adipose tissue images of adipocyte area (A) and adipocyte size frequency distribution (B, C) at 3 and 6 h post-injection with PBS (control, white bars/black triangles) or λ-carrageenin (1%, blue bars/blue squares). The error bars in the columns denote the standard error of the means (n = 7). Asterisks indicate significant differences between control and λ-carrageenin groups (*t*-test; $p < 0.05$).

embedding process (Fig. 1). Quantitative analysis of adipocytes revealed a statistically significant ($p < 0.05$) increase in the area of adipocytes present in the subepidermal fat of fish injected with λ-carrageenin and sampled 3 h p.i., compared with the adipocyte area of fish in the control group (injected with PBS) (Fig. 2). However, adipocyte frequency was not statistically significantly altered in carrageenin-injected fish sampled 3 h p.i. compared with the control (Fig. 2B). Otherwise, although the adipocyte area of fish in the λ-carrageenin group at 6 h remained unchanged with respect to fish injected with PBS at the same time, the frequency of adipocytes in the interval between 4500 and 5000 μm^2 was increased in the skin of fish from the λ-carrageenin-injected group sampled 6 h p.i. ($p < 0.05$), compared with the value obtained in adipocytes in the fat of fish in the control group sampled at the same time (Fig. 2C).

3.2. Lipid analysis

3.2.1. Lipid class analysis

No differences in total polar or neutral lipids were observed at either 3 or 6 h after carrageenin injection compared with the control group (Fig. 3A and B). However, this analysis indicated a higher FFA content in skin samples of fish injected with λ-carrageenin and sampled at 3 h p.i. (although not at 6 h) compared with the FFA content in the skin of fish from the control group (Fig. 3C). In terms of time, FFA content decreased in the skin of fish at 6 h p.i. with λ-carrageenin compared with fish sampled 3 h p.i. This lipid class was the only one in which an interaction between treatment and time was observed (Table 3).

Furthermore, no changes in SM content were observed in skin samples from fish injected with λ-carrageenin or PBS and sampled at 3 h p.i. However, higher SM content was detected in skin samples from fish injected with λ-carrageenin and sampled at 6 h p.i. compared with fish injected with PBS and sampled at the same time (Fig. 3D).

3.2.2. Fatty acid methyl esters analysis

Analysis of FAMEs showed no statistical variations in skin samples evaluated at 3 h p.i. between control fish and those in the λ-carrageenin-injected group (Fig. 4). However, an increase in total SFAs and total n-6 PUFAs (22:4n-6) was observed in carrageenin-injected fish sampled at 6 h p.i. compared with the control group (Fig. 5). The fatty acids that increased were mainly represented by SFAs 18:0, 20:0 and 24:0 (Fig. 5B), and n-6 PUFAs 18:2n-6 and 22:4n-6, respectively (Fig. 5C). In contrast, in the skin of fish injected with λ-carrageenin and sampled at 6 h p.i. we observed a decrease in MUFAs (20:1n-11, 22:1n-11 and 22:1n-9, Fig. 5D), n-3 PUFAs (18:3n-3, 18:4n-3 and 20:4n-3, Fig. 5E) and a decrease of 16:2 (Fig. 5F), compared to the values obtained in fish from the control group and sampled at 6 h p.i. Considering time, a decrease in 18:3n-3 content was detected in both PBS and λ-carrageenin groups at 6 h p.i. compared to the values found at 3 h p.i. (Table 4). In addition, the levels of 20:3n-3 and 20:4n-3 were decreased at 6 h p.i. in fish injected with PBS compared to the values observed in the skin of the same group of fish studied at 3 h p.i. Likewise, the level of 18:4n-3 decreased at 6 h p.i. in the group of fish injected with λ-carrageenin compared to the same group at 3 h p.i(see Table 5).

3.2.3. Eicosanoid analysis

Regarding eicosanoids analysis (Fig. 6), no significant variations were detected in the levels of skin samples from fish of both groups, carrageenin and control, at 3 h p.i. (Fig. 6A). However, the level of 5-HETE increased in the skin of fish injected with λ-carrageenin sampled at 6 h p.i. compared with the control group (Fig. 6B). Taking into account the time factor, the levels of 17-HpDHA and 14-HDHA decreased at 6 h p.i. in the with PBS and λ-carrageenin injected fish group, respectively, compared with the same groups studied at 3 h p.i. (Table 4).

3.3. Gene expression analysis

The expression profile of three proinflammatory cytokines and three molecules involved in adipocyte lipid metabolism was analysed by real-time PCR in fish skin samples collected 1.5, 3 and 6 h after carrageenan or PBS (control) injection. The results are shown in Supplementary Fig. 1. No gene expression was altered in skin samples collected 1.5 h after carrageenan injection compared to the expression values obtained in fish injected with PBS (control). However, the expression of the proinflammatory genes *il1b, tnfa,* and *il6* was significantly increased in the skin of fish injected with carrageenan and sampled after 3 h p.i., compared with the values of fish in the control group (Fig. S1A- S1C). In addition, the expression of the cytokines *tnfa* and *il6* remained significantly increased in fish injected with carrageenan and sampled at 6 h after injection. Similarly, gene expression of the adipokine *lepa* was also up-regulated at 6 h after carrageenan injection compared to the control

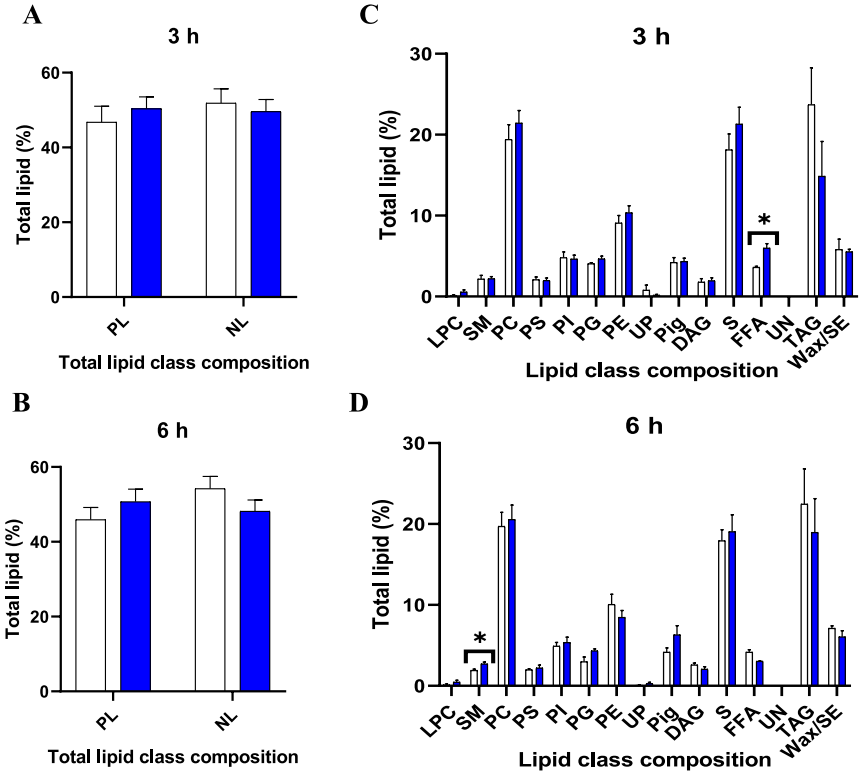

Fig. 3. Lipid class analysis of gilthead seabream skin samples at 3 (A) and 6 h (B) after injection with PBS (control, white bars) or λ-carrageenin (1%, blue bars). Error bars in the columns indicate standard error of means (n = 7). Asterisks indicate significant differences between control and λ-carrageenin groups (*t*-test; $p < 0.05$).

Table 3
Lipid class analysis of gilthead seabream skin samples at 3 and 6 h post-injection with PBS or λ-carrageenin. Asterisks indicate interaction between the experimental factors (Treatment*Time) (Two-way-ANOVA; $p < 0.05$) and significant differences between time points (*t*-test; $p < 0.05$).

Lipid class	Treatment*Time	Treatment	Time (3 h–6 h)
Total Polar	–	PBS	–
		λ-carrageenin	–
Total Neutral	–	PBS	–
		λ-carrageenin	–
LPC	–	PBS	–
		λ-carrageenin	–
SM	–	PBS	–
		λ-carrageenin	–
PC	–	PBS	–
		λ-carrageenin	–
PS	–	PBS	–
		λ-carrageenin	–
PI	–	PBS	–
		λ-carrageenin	–
PG	–	PBS	–
		λ-carrageenin	–
PE	–	PBS	–
		λ-carrageenin	–
UP	–	PBS	–
		λ-carrageenin	–
Pig	–	PBS	–
		λ-carrageenin	–
DAG	–	PBS	–
		λ-carrageenin	–
S	–	PBS	–
		λ-carrageenin	–
FFA	*	PBS	–
		λ-carrageenin	*
UN	–	PBS	–
		λ-carrageenin	–
TAG	–	PBS	–
		λ-carrageenin	–
Wax/SE	–	PBS	–
		λ-carrageenin	–

group (Fig. S1D). Interestingly, no significant variations in *lepb* and *pparg* gene expression were observed in fish injected with carrageenan or PBS compared to control levels at any experimental time point (Fig. S1E-S1F).

Considering the time factor, although no statistical differences were found in the expression of any gene studied in the control group fish, gene expression of *il6* and *lepa* was up-regulated at 6 h post carrageenan injection compared to the values found at 1.5 h and 6 p.i. (Figs. S1C and S1D).

4. Discussion

In previous studies, the intramuscular injection of 1% carrageenin in PBS (50 μL per fish) in the left flank of gilthead seabream, below the lateral line at the level of the second dorsal fin, triggered acute skin inflammation with a peak at 3 h after administration, which then began to resolve after 6 h [36,37]. In this study, the expression of three proinflammatory cytokines and three molecules involved in the lipid metabolism of adipocytes has been studied. The results indicate that, as had already been shown in previous studies, the proinflammatory genes *il1b, tnfa,* and *il6* increased their expression in the skin of fish injected with carrageenan and sampled 3 h p.i., compared to the values of the control group fish. In addition, the expression of *tnfa* and *il6* continued to be significantly increased in fish injected with carrageenan and sampled at 6 h p.i. Of the three adipokines studied, only *lepa* expression was significantly increased in fish injected with carrageenan and sampled at 6 h p.i. 6 h p.i., compared to the control group. In addition, although carrageenin injection had no impact on systemic immunity of gilthead seabream, it led to an increase in the number of skin mucus-secreting cells and acidophilic granulocytes, as well as up-regulation of proinflammatory genes in the skin near the injection site [38,40]. These events were associated with increased skin thickness, edema, and emphysema in the underlying muscle, which were the symptoms observed in human necrotizing fasciitis [39]. Considering the localized effects caused by carrageenin injection, in the present study we

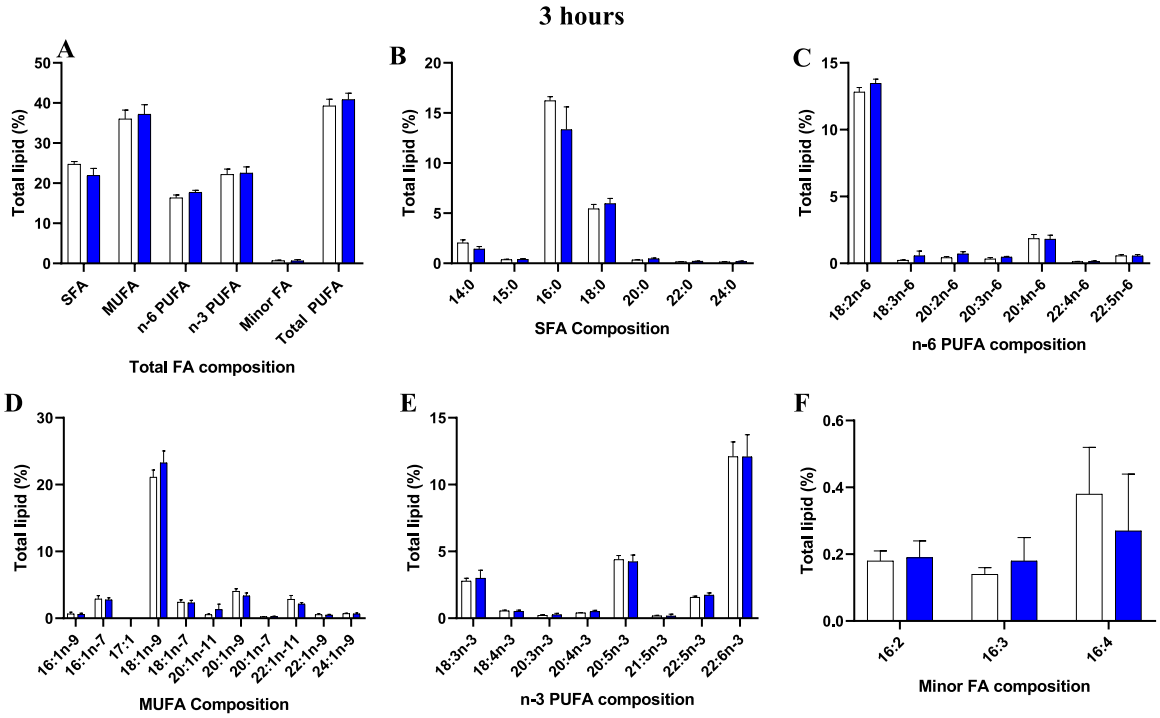

Fig. 4. Analysis of fatty acid methyl esters (FAMEs) in gilthead seabream skin samples at 3 h post-injection with PBS (control, white bars) or λ-carrageenin (1%, blue bars). Total fatty acid (FA) composition (A), saturated FA (SFA) composition (B), n-6 polyunsaturated FA (PUFA) composition (C), monounsaturated FA (MUFA) composition (D), n-3 PUFA composition (E) and minor FA composition (F). Error bars in the columns indicate the standard error of the means (n = 7)..

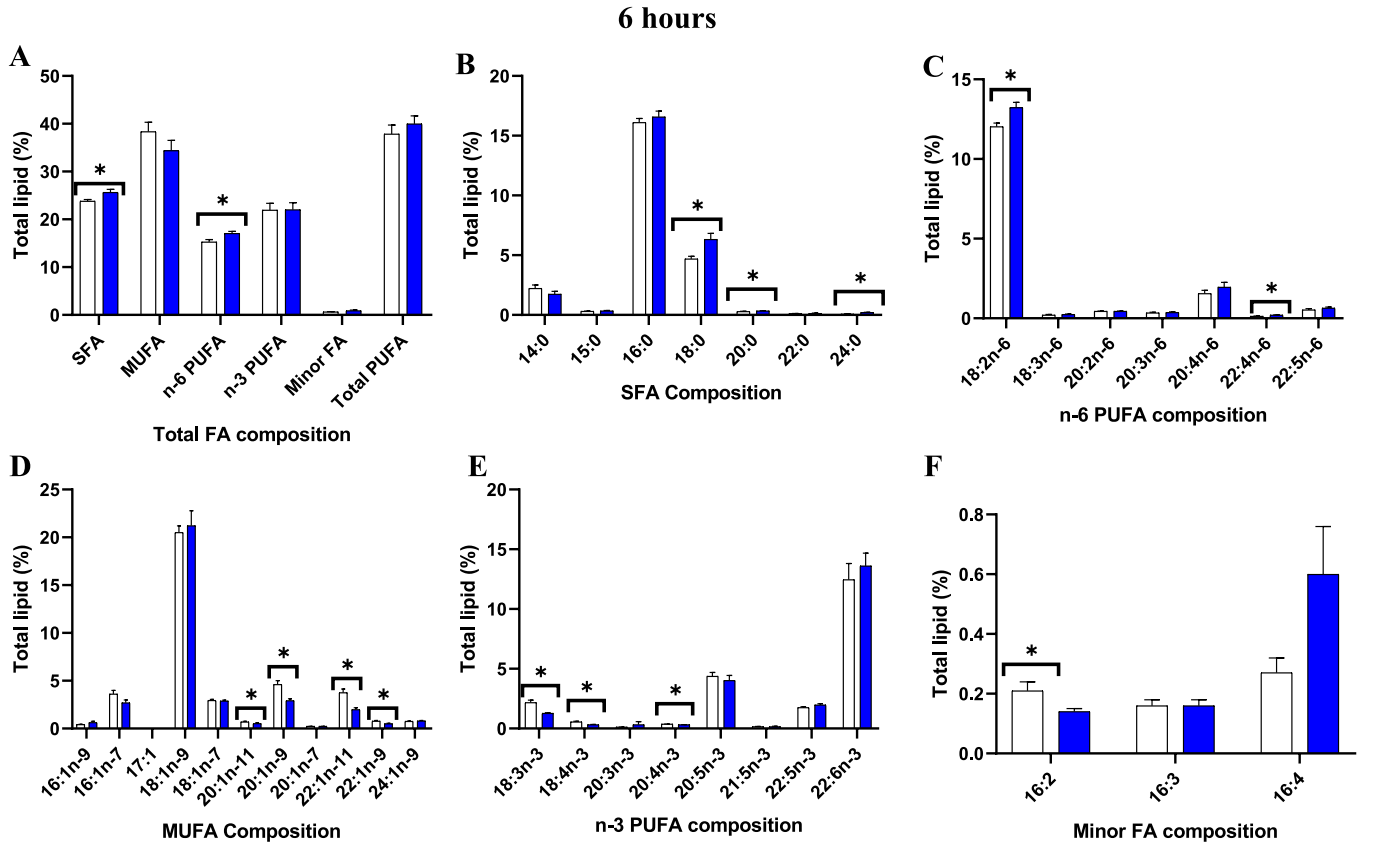

Fig. 5. Analysis of fatty acid methyl esters (FAMEs) in gilthead seabream skin samples at 6 h post-injection with PBS (control, white bars) or λ-carrageenin (1%, blue bars). Total fatty acid (FA) composition (A), saturated FA (SFA) composition (B), n-6 polyunsaturated FA (PUFA) composition (C), monounsaturated FA (MUFA) composition (D), n-3 PUFA composition (E) and minor FA composition (F). Error bars in the columns indicate the standard error of the means (n = 7). Asterisks indicate significant differences between control and λ-carrageenin groups (*t*-test; $p < 0.05$).

want to delve deeper into the events taking place at the injection site. To the best of our knowledge, this is the first study to evaluate the role of subcutaneous adipose tissue adipocytes and fatty acids in fish skin inflammation.

The interest of adipocytes lies in their function of regulating energy balance, storing FAs in the form of TAGs during periods of energy excess and releasing them when needed. In a state of negative energy balance, TAGs are hydrolysed to FFAs and glycerol (lipolysis), the FFAs being transported to the required organs where they will be used for energy production through β-oxidation [49]. On the other hand, in a positive energy balance, adipocytes can re-esterify FFA to accumulate them, thus increasing their size (hypertrophy), or differentiate from undifferentiated mesenchymal stem cells (MSCs) into preadipocytes and mature adipocytes (hyperplasia) to also increase the size of ATs [50,51]. All these processes are highly regulated by nutritional factors, cytokines and hormones in both fish and mammals [52–54]. However, some dysregulation in adipocyte metabolism could lead to altered fish health associated with fat deposition [55]. According to our histological study, an increase in adipocyte area in SAT was detected in fish injected with λ-carrageenin at 3 h p.i. These results could be the morphological evidence of the response of adipocytes to the proinflammatory mediators that are released, in the area of inflammation, by immune cells recruited at this time point (3 h) [36,38,40]. This morphological change could be necessary to induce the polarization of adipocytes in the inflamed zone towards a proinflammatory phenotype. This hypothesis could make sense since, according to some *in vitro* studies, human and mammalian adipocytes are able to produce proinflammatory cytokines [56,57], express chemokines [58], innate immune receptors [59–61], and present antigens to immune cells [62–64], directly modulating the inflammatory response. Our results are also in agreement with studies developed in rodents, which explain that hypertrophic adipocytes and excessive fat accumulation (i.e., obesity), are accompanied by the recruitment of immune cells such as macrophages in the AT [65,66]. In our study, the content of n-6 PUFAs 18:2n-6 (linoleic acid) and 22:4n-6 (adrenic acid), and the content of n-3 PUFAs 18:3n-3 (α-linolenic acid), 18:4n-3 (stearidonic acid) and 20:4n-3 (eicosatetraenoic acid), increased and decreased, respectively, in the skin of fish sampled at 6 h post-carrageenin injection compared to the control group. Interestingly, immune cell membranes are constituted by phospholipids with a high content of n-6 PUFAs and a low content of n-3 PUFAs [13]. These results could also support the recruitment of immune cells at the inflammation zone at this experimental time (6 h), previously evidenced by our research group by histology and gene expression analysis [36,40]. Besides this, the presence of n-3 PUFAs has been associated with the activation of PPAR-γ, the subsequent inhibition of NF-κB (the main molecular regulator of inflammation), and therefore, with the reduction of the inflammatory response [13]. The decrease of n-3 PUFAs evidenced in skin samples obtained at 6 h p.i. in the λ-carrageenin group compared to the control group would indicate that carrageenin might be able to activate some proinflammatory mechanism to prolong the acute inflammatory reaction up to this time. In this regard, the roles of MUFAs in inflammation are less well documented, but like the n-3 PUFAs, evidence also links MUFAs to anti-inflammatory states [67]. In the present study, the decrease in MUFAs, specifically 20:1n-11 (eicosenoic acid), 20:1n-9 (gondoic acid), 22:1n-11 (ketoleic acid) and 22:1n-9 (erucic acid) evidenced in fish injected with λ-carrageenin and sampled at 6 h p.i. compared to control fish could support the above hypothesis. Moreover, the decrease in both types of FAs (MUFAs and n-3 PUFAs) could

Table 4
Analysis of fatty acid methyl esters (FAMEs) in gilthead seabream skin samples at 3 and 6 h post-injection with PBS or λ-carrageenin. Asterisks indicate interaction between the experimental factors (Treatment*Time) (Two-way-ANOVA; $p < 0.05$) and significant differences between time points (*t*-test; $p < 0.05$).

FAMEs	Treatment*Time	Treatment	Time (3 h–6 h)
SFA	–	PBS	–
		λ-carrageenin	–
MUFA	–	PBS	–
		λ-carrageenin	–
n-6 PUFA	–	PBS	–
		λ-carrageenin	–
n-3 PUFA	–	PBS	–
		λ-carrageenin	–
Minor FA	–	PBS	–
		λ-carrageenin	–
Total PUFA	–	PBS	–
		λ-carrageenin	–
14:0	–	PBS	–
		λ-carrageenin	–
16:0	–	PBS	–
		λ-carrageenin	–
18:0	–	PBS	–
		λ-carrageenin	–
20:0	–	PBS	–
		λ-carrageenin	–
20:0	–	PBS	–
		λ-carrageenin	–
22:0	–	PBS	–
		λ-carrageenin	–
24:0	–	PBS	–
		λ-carrageenin	–
18:2n-6	–	PBS	–
		λ-carrageenin	–
18:3n-6	–	PBS	–
		λ-carrageenin	–
20:2n-6	–	PBS	–
		λ-carrageenin	–
20:3n-6	–	PBS	–
		λ-carrageenin	–
20:4n-6	–	PBS	–
		λ-carrageenin	–
22:4n-6	–	PBS	–
		λ-carrageenin	–
22:5n-6	–	PBS	–
		λ-carrageenin	–
16:1n-9	–	PBS	–
		λ-carrageenin	–
16:1n-7	–	PBS	–
		λ-carrageenin	–
17:1	–	PBS	–
		λ-carrageenin	–
18:1n-9	–	PBS	–
		λ-carrageenin	–
18:1n-7	–	PBS	–
		λ-carrageenin	–
20:1n-11	–	PBS	–
		λ-carrageenin	–
20:1n-9	–	PBS	–
		λ-carrageenin	–
20:1n-7	–	PBS	–
		λ-carrageenin	–
22:1n-11	–	PBS	–
		λ-carrageenin	–
22:1n-9	–	PBS	–
		λ-carrageenin	–
24:1n-9	–	PBS	–
		λ-carrageenin	–
18:3n-3	–	PBS	*
		λ-carrageenin	*
18:4n-3	–	PBS	–
		λ-carrageenin	*
20:3n-3	–	PBS	*
		λ-carrageenin	–
20:4n-3	–	PBS	*
		λ-carrageenin	–
20:5n-3	–	PBS	–
		λ-carrageenin	–
21:5n-3	–	PBS	–
		λ-carrageenin	–
22:5n-3	–	PBS	–
		λ-carrageenin	–
22:6n-3	–	PBS	–
		λ-carrageenin	–
16:2	–	PBS	–
		λ-carrageenin	–
16:3	–	PBS	–
		λ-carrageenin	–
16:4	–	PBS	–
		λ-carrageenin	–

Table 5
Eicosanoid analysis in gilthead seabream skin samples at 3 and 6 h post-injection with PBS or λ-carrageenin. Asterisks indicate interaction between the experimental factors (Treatment*Time) (Two-way-ANOVA; $p < 0.05$) and significant differences between time points (*t*-test; $p < 0.05$).

Lipid class	Treatment*Time	Treatment	Time (3 h–6 h)
13-HOTrE	–	PBS	–
		λ-carrageenin	–
9-HODE	–	PBS	–
		λ-carrageenin	–
13-HODE	–	PBS	–
		λ-carrageenin	–
5-HEPE	–	PBS	–
		λ-carrageenin	–
12-HEPE	–	PBS	–
		λ-carrageenin	–
15-HEPE	–	PBS	–
		λ-carrageenin	–
5-HETE	–	PBS	–
		λ-carrageenin	–
12-HETE	–	PBS	–
		λ-carrageenin	–
15-HETE	–	PBS	–
		λ-carrageenin	–
15-HETrE	–	PBS	–
		λ-carrageenin	–
5,15-diHETE	–	PBS	–
		λ-carrageenin	–
17-HpDHA	–	PBS	*
		λ-carrageenin	–
14-HDHA	–	PBS	–
		λ-carrageenin	*
17-HDHA	–	PBS	–
		λ-carrageenin	–

point to the redistribution and utilization of these fatty acids for their synthesis or reconversion into other molecules, avoiding excessive energy expenditure. Likewise, λ-carrageenin-activated adipocytes could contribute to the inflammatory process through the production of molecules with inflammatory functions derived from the hydrolysis of TAGs to FFA, as well as directly synthesizing FFA *de novo* (lipogenesis) [11,68,69]. The latter fact would explain the increase in FFA content detected at 3 h p.i. in the skin samples of fish injected with λ-carrageenin, but with no change in TAG content between experimental groups. Thus, it has been shown that FFA act as stress-inducing molecules in mammalian macrophages that are able to activate NF-κB through TLR-4, as well as to impair the integrity of organelles such as mitochondria and lysosomes, generating radical oxygen species [70]. Furthermore, among the different products into which FFAs can be metabolized, SFAs, such as lauric acid (12:0), have also been shown to potentiate at the molecular level the activation of NF-κB through TLR-4 in mammalian macrophages [71]. This event seems to be somehow related to the promotion or disruption of the raft formation in adipocyte membranes and, therefore, to the activation or inhibition of the inflammatory process. However, the

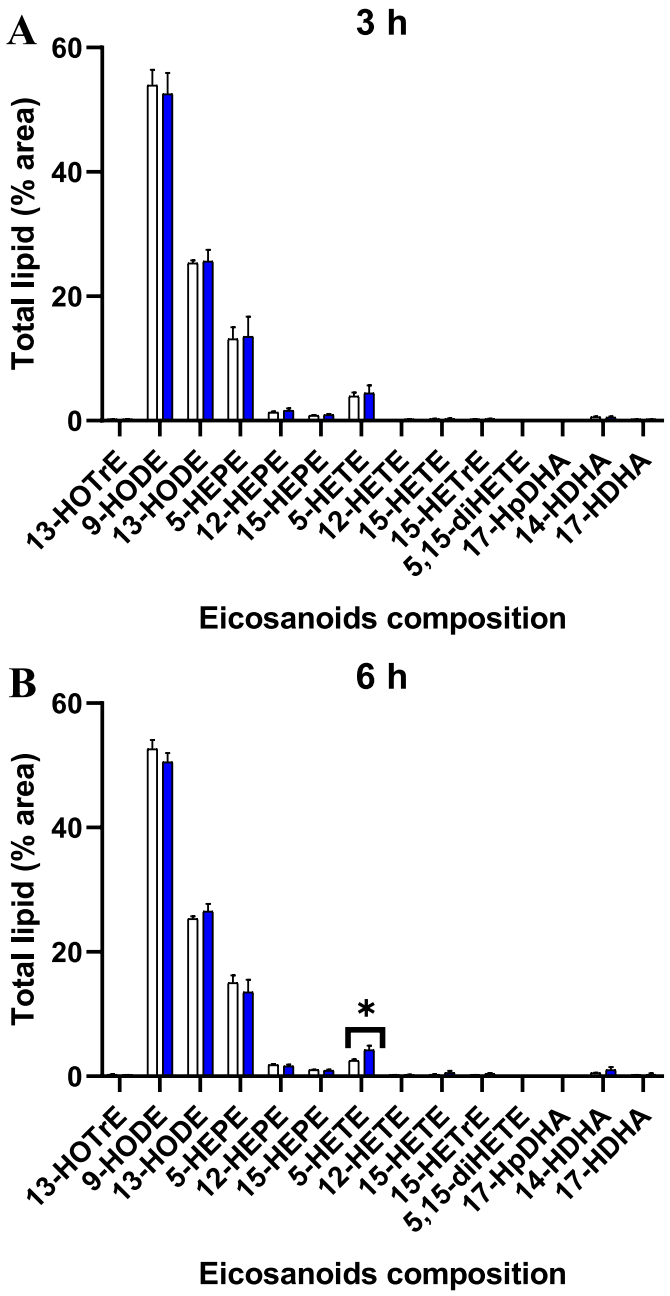

Fig. 6. Eicosanoid analysis in gilthead seabream skin samples at 3 (A) and 6 (B) h post-injection with PBS (control, white bars) or λ-carrageenin (1%, blue bars). Error bars in the columns indicate standard error of means (n = 7). Asterisk indicates significant differences between control and λ-carrageenin groups (*t*-test; $p < 0.05$).

role of SFAs is of such magnitude that elevated levels of SFAs in the human diet can be considered a proinflammatory factor in itself. According to our study, SFAs 18:0 (stearic acid), 20:0 (arachidic acid) and 24:0 (lignoceric/tetracosanoic acid) increased their content in skin samples obtained 6 h p.i. with λ-carrageenin, which could indicate the role of SFAs in activating inflammation. In addition, and taking into account that the presence of TLR4 orthologs are unknown in gilthead seabream [72], different SFAs such as those detected in this study could be produced to activate different inflammatory cascades, probably contributing to the activation and recruitment of immune cells.

According to our histological study, the frequency of adipocytes with an area of 4500–5000 μm^2 was increased at 6 h p.i. in fish injected with λ-carrageenin, which could also point to the activation of a regulatory mechanism that stabilises the size of these cells and prevents their continuous growth, preventing excessive inflammation. In addition, a higher SM content was detected in skin samples from fish in the λ-carrageenin group and sampled at 6 h p.i. compared to fish injected with PBS and sampled at the same time. SMs are sphingolipids that are mainly concentrated in the caveolae of the cell membrane of adipocytes and in the lipid rafts of macrophages, in both cases performing specialized functions that can modulate the inflammatory response [73,74]. These functions could include cell signalling, and participation in clathrin-independent processes of endocytosis, phagocytosis and apoptosis [73,74]. Thus, the function of SM could be linked to the activation of regulatory mechanisms such as apoptosis of immune cells that have already fulfilled their function at the site of inflammation to avoid excessive inflammation, and their subsequent elimination by phagocytosis.

As for other mediators and regulators of inflammation, such as eicosanoids, which are key in mammals, in our study only the level of 5-HETE at 6 h p.i. was increased in the skin of fish in the λ-carrageenin group compared to the control group. These results are in agreement with previous data pointing to a secondary role of eicosanoids in the inflammatory pathway in seabream induced by carrageenin compared to mammals, at least at these experimental time points [40]. Thus, not only the timing of eicosanoid production and the concentrations of the different eicosanoids, but also the sensitivity of the target cells and tissues to the eicosanoids generated, could be some of the particularities to be taken into account to explain this major difference in gilthead seabream relative to mammals [13].

On the other hand, 5-HETE is a precursor molecule of other leukotrienes, and it is released by degranulation of mammalian neutrophils (acidophilic granulocytes in gilthead seabream) upon bacterial infections or stimulation with lipopolysaccharide [75]. Interestingly, acidophilic granulocytes seem to be the main cells involved in this inflammatory process according to our previous data [40]. The increase of 5-HETE could serve as an autocrine and paracrine mechanism of these cells in order to modulate the acute inflammation.

In conclusion, the present results seem to indicate that one intramuscular injection of λ-carrageenin is able to produce an acute inflammatory reaction in gilthead seabream leading to relevant changes in the adipocytes morphology and function, as well as in FA metabolism. The present data point to adipocytes are a very flexible and modulable cells with immune-like functions. In this sense adipocytes are able to contribute to the inflammatory response triggered by λ-carrageenin, as well as to participate in its regulation and termination by modulating their FA metabolism as a function of energy balance. Our findings provide a new approach to the local inflammatory mechanisms evolved by carrageenin in a fish species with a high commercial interest.

CRediT authorship contribution statement

Jose Carlos Campos-Sánchez: Methodology, Formal analysis, Investigation, Writing – original draft, Writing – review & editing, Visualization. **Daniel Gonzalez-Silvera:** Methodology, Investigation, Writing – review & editing, Visualization. **Xu Gong:** Methodology, Validation, Investigation, Writing – review & editing, Visualization. **Richard Broughton:** Methodology, Validation, Investigation, Writing – review & editing, Visualization. **Francisco A. Guardiola:** Writing – review & editing, Visualization. **Mónica B. Betancor:** Conceptualization, Formal analysis, Data curation, Writing – original draft, Writing – review & editing, Visualization, Supervision. **María Ángeles Esteban:** Term, Conceptualization, Resources, Writing – review & editing, Visualization, Supervision, Project administration, Funding acquisition.

Data availability

Data will be made available on request.

Acknowledgements

This work was financed by the Spanish project *PID2020-113637RB-C21 financiado por MCIN/AEI*, by *the Comunidad Autónoma Región de Murcia-Fundación Séneca (ThinkInAzul). España. Unión europea*", and by the Program Moving Minds (R-173/2022) of the Vice Rectorate of Internationalization of the University of Murcia.

Appendix A. Supplementary data

Supplementary data to this article can be found online at https://doi.org/10.1016/j.fsi.2022.09.066.

References

[1] G.Y. Chen, G. Nuñez, Sterile inflammation: sensing and reacting to damage, Nat. Rev. Immunol. 10 (2010) 826–837, https://doi.org/10.1038/nri2873.
[2] R. Medzhitov, Origin and physiological roles of inflammation, Nature 454 (2008) 428–435, https://doi.org/10.1038/nature07201.
[3] P.M. Henson, Dampening inflammation, Nat. Immunol. 6 (2005) 1179–1181.
[4] C. Nathan, A. Ding, Nonresolving inflammation, Cell 140 (2010) 871–882, https://doi.org/10.1016/j.cell.2010.02.029.
[5] P.C. Calder, N. Ahluwalia, R. Albers, N. Bosco, R. Bourdet-Sicard, D. Haller, S. T. Holgate, L.S. Jönsson, M.E. Latulippe, A. Marcos, J. Moreines, C. Mrini, M. Müller, G. Pawelec, R.J.J. Van Neerven, B. Watzl, J. Zhao, A consideration of biomarkers to be used for evaluation of inflammation in human nutritional studies, Br. J. Nutr. 109 (2013), https://doi.org/10.1017/S0007114512005119.
[6] C.N. Sarantopoulos, D.A. Banyard, M.E. Ziegler, B. Sun, A. Shaterian, A. D. Widgerow, Elucidating the preadipocyte and its role in adipocyte formation: a comprehensive review, Stem Cell Rev. Reports. 14 (2018) 27–42, https://doi.org/10.1007/s12015-017-9774-9.
[7] C.C. Chan, M.S.M.A. Damen, P.C. Alarcon, J. Sanchez-Gurmaches, S. Divanovic, Inflammation and immunity: from an adipocyte's perspective, J. Interferon Cytokine Res. 39 (2019) 459–471, https://doi.org/10.1089/jir.2019.0014.
[8] C.C. Chan, M.S.M.A. Damen, M.E. Moreno-Fernandez, T.E. Stankiewicz, M. Cappelletti, P.C. Alarcon, J.R. Oates, J.R. Doll, R. Mukherjee, X. Chen, R. Karns, M.T. Weirauch, M.A. Helmrath, T.H. Inge, S. Divanovic, Type I interferon sensing unlocks dormant adipocyte inflammatory potential, Nat. Commun. 11 (2020) 1–15, https://doi.org/10.1038/s41467-020-16571-4.
[9] M.S. Han, A. White, R.J. Perry, J.P. Camporez, J. Hidalgo, G.I. Shulman, R.J. Davis, Regulation of adipose tissue inflammation by interleukin 6, Proc. Natl. Acad. Sci. U.S.A. 117 (2020) 2751–2760, https://doi.org/10.1073/pnas.1920004117.
[10] N. Ouchi, J.L. Parker, J.J. Lugus, K. Walsh, Adipokines in inflammation and metabolic disease, Nat. Rev. Immunol. 11 (2011) 85–97, https://doi.org/10.1038/nri2921.
[11] M. Lafontan, D. Langin, Lipolysis and lipid mobilization in human adipose tissue, Prog. Lipid Res. 48 (2009) 275–297, https://doi.org/10.1016/j.plipres.2009.05.001.
[12] P. Dandona, A. Aljada, S. Dhindsa, D. Tripathy, P. Mohanty, H. Ghanim, T. Syed, Elevation of free fatty acids induces inflammation and impairs vascular reactivity in healthy subjects, Diabetes 52 (2007) 2882–2887.
[13] P.C. Calder, Fatty acids and inflammation: the cutting edge between food and pharma, Eur. J. Pharmacol. 668 (2011), https://doi.org/10.1016/j.ejphar.2011.05.085. S50–S58.
[14] G. Schmitz, J. Ecker, The opposing effects of n-3 and n-6 fatty acids, Prog. Lipid Res. 47 (2008) 147–155, https://doi.org/10.1016/j.plipres.2007.12.004.
[15] R.A. Lewis, K.F. Austen, R.J. Soberman, Leukotrienes and other products of the 5-lipoxygenase pathway: biochemistry and relation to pathobiology in human diseases, New English J. Med. 323 (1990) 1120–1123.
[16] S.L. Tilley, T.M. Coffman, B.H. Koller, Mixed messages: modulation of inflammation and immune responses by prostaglandins and thromboxanes, J. Clin. Invest. 108 (2001) 15–23, https://doi.org/10.1172/JCI200113416.
[17] C.L. Pratt, C.R. Brown, The role of eicosanoids in experimental Lyme arthritis, Front. Cell. Infect. Microbiol. 4 (2014) 1–6, https://doi.org/10.3389/fcimb.2014.00069.
[18] J. Necas, L. Bartosikova, Carrageenan: a review, Vet. Med. (Praha) 58 (2013) 187–205, https://doi.org/10.17221/6758-VETMED.
[19] C.A. Winter, E.A. Risley, G.W. Nuss, Carrageenin-induced edema in hind paw of the rat as an assay for antiinflammatory drugs, Proc. Soc. Exp. Biol. Med. 111 (1962) 544–547.
[20] C.J. Morris, Carrageenan-induced paw edema in the rat and mouse, Methods Mol. Biol. 225 (2003) 115–121, https://doi.org/10.1385/1-59259-374-7:115.
[21] L. Levy, Carrageenan paw edema in the mouse, Life Sci. 8 (1969) 601–606, https://doi.org/10.1016/0024-3205(69)90021-6.
[22] S. Bhattacharyyaa, H. Liu, Z. Zhang, M. Jam, P.K. Dudeja, G. Michel, R. Linhardt, J. K. Tobacman, Carrageenan-induced innate immune response is modified by enzymes that hydrolyze distinct galactosidic Bonds, J. Nutr. Biochem. 21 (2010) 906–913, https://doi.org/10.1038/jid.2014.371.
[23] K. Fujiki, D. Shin, M. Nakao, T. Yano, Effects of κ-carrageenan on the non-specific of carp *Cyprinus carpio*, Fish. Sci. 63 (1997) 934–938.
[24] E.V. Sokolova, L.N. Bogdanovich, T.B. Ivanova, A.O. Byankina, S.P. Kryzhanovskiy, I.M. Yermak, Effect of carrageenan food supplement on patients with cardiovascular disease results in normalization of lipid profile and moderate modulation of immunity system markers, PharmaNutrition 2 (2014) 33–37, https://doi.org/10.1016/j.phanu.2014.02.001.
[25] N. Das, A. Kumar, R.G. Rayavarapu, The role of deep eutectic solvents and carrageenan in synthesizing biocompatible anisotropic metal nanoparticles, Beilstein J. Nanotechnol. 12 (2021) 924–938, https://doi.org/10.3762/bjnano.12.69.
[26] S. García-Poza, A. Leandro, C. Cotas, J. Cotas, J.C. Marques, L. Pereira, A.M. M. Gonçalves, The Evolution Road of Seaweed Aquaculture: Cultivation Technologies and the Industry, 4.0, 2020, https://doi.org/10.3390/ijerph17186528.
[27] C.E. Boyd, A.A. McNevin, R.P. Davis, The contribution of fisheries and aquaculture to the global protein supply, Food Secur. 14 (2022) 805–827, https://doi.org/10.1007/s12571-021-01246-9.
[28] M. Younes, P. Aggett, F. Aguilar, R. Crebelli, M. Filipič, M.J. Frutos, P. Galtier, D. Gott, U. Gundert-Remy, G.G. Kuhnle, C. Lambré, J.C. Leblanc, I.T. Lillegaard, P. Moldeus, A. Mortensen, A. Oskarsson, I. Stankovic, I. Waalkens-Berendsen, R. A. Woutersen, M. Wright, L. Brimer, O. Lindtner, P. Mosesso, A. Christodoulidou, S. Ioannidou, F. Lodi, B. Dusemund, Re-evaluation of carrageenan (E 407) and processed Eucheuma seaweed (E 407a) as food additives, EFSA J. 16 (2018), https://doi.org/10.2903/j.efsa.2018.5238.
[29] M. Timur, R.J. Roberts, A. McQueen, Carrageenin granuloma in the plaice (*Pleuronectes platessa*); a histopathological study of chronic inflammation in a teleost fish, J. Comp. Pathol. 87 (1977) 89–96.
[30] E. Matushima, M. Mariano, Kinetics of the inflammatory reaction induced by carrageenin in the swimbladder of *Oreochromis niloticus* (Nile tilapia), Braz. J. Vet. Res. Anim. Sci. 33 (1996) 5–10.
[31] M. Martins, D. Myiazaki, M. Tavares-Dias, J. Fenerick Jr., E. Onaka, F. Bozzo, R. Fujimoto, F. Moraes, Characterization of the acute inflammatory response in the hybrid tambacu (*Piaractus mesopotamicus* male × *Colossoma macropomum* female) (Osteichthyes), Braz. J. Biol. 69 (2009) 957–962, https://doi.org/10.1590/s1519-69842009000400026.
[32] M.L. Martins, F.R. De Moraes, R.Y. Fujimoto, E.M. Onaka, F.R. Bozzo, J.R.E. De Moraes, Carrageenin induced inflammation in *Piaractus mesopotamicus* (osteichthyes : characidae) cultured in Brazil, B. Inst. Pesca. 32 (2006) 31–39.
[33] S.Y. Huang, C.W. Feng, H.C. Hung, C. Chakraborty, C.H. Chen, W.F. Chen, Y. H. Jean, H.M.D. Wang, C.S. Sung, Y.M. Sun, C.Y. Wu, W. Liu, C. Der Hsiao, Z. H. Wen, A novel zebrafish model to provide mechanistic insights into the inflammatory events in carrageenan-induced abdominal edema, PLoS One 9 (2014), https://doi.org/10.1371/journal.pone.0104414.
[34] J.L.C. Ribas, A.R. Zampronio, H.C. Silva de Assis, Effects of trophic exposure to diclofenac and dexamethasone on hematological parameters and immune response in freshwater fish, Environ. Toxicol. Chem. 35 (2016) 975–982, https://doi.org/10.1002/etc.3240.
[35] M.A.A. Belo, M.F. Oliveira, S.L. Oliveira, M.F. Aracati, L.F. Rodrigues, C.C. Costa, G. Conde, J.M.M. Gomes, M.N.L. Prata, A. Barra, T.M. Valverde, D.C. de Melo, S. F. Eto, D.C. Fernandes, M.G.M.C. Romero, J.D. Corrêa Júnior, J.O. Silva, A.L. B. Barros, A.C. Perez, I. Charlie-Silva, Zebrafish as a model to study inflammation: a tool for drug discovery, Biomed. Pharmacother. 144 (2021), https://doi.org/10.1016/j.biopha.2021.112310.
[36] J.C. Campos-Sánchez, J. Mayor-Lafuente, D. González-Silvera, F.A. Guardiola, M.Á. Esteban, Acute inflammatory response in the skin of gilthead seabream (*Sparus aurata*) caused by carrageenin, Fish Shellfish Immunol. 119 (2021) 623–634, https://doi.org/10.1016/j.fsi.2021.10.009.
[37] J.C. Campos-Sánchez, J. Mayor-Lafuente, F.A. Guardiola, M.Á. Esteban, *In silico* and gene expression analysis of the acute inflammatory response of gilthead seabream (*Sparus aurata*) after subcutaneous administration of carrageenin, Fish Physiol. Biochem. (2021), https://doi.org/10.1007/s10695-021-00999-6.
[38] J.C. Campos-Sánchez, F.A. Guardiola, J.M. García Beltrán, D. Ceballos-Francisco, M.Á. Esteban, Effects of subcutaneous injection of λ/κ-carrageenin on the immune and liver antioxidant status of gilthead seabream (*Sparus aurata*), J. Fish. Dis. 44 (2021) 1449–1462, https://doi.org/10.1111/jfd.13452.
[39] J.C. Campos-Sánchez, N.G. Carrillo, F.A. Guardiola, D.C. Francisco, M.Á. Esteban, Ultrasonography and X-ray micro-computed tomography characterization of the effects caused by carrageenin in the muscle of gilthead seabream (*Sparus aurata*), Fish Shellfish Immunol. 123 (2022) 431–441, https://doi.org/10.1016/j.fsi.2022.03.013.
[40] J.C. Campos-Sánchez, E. Vitarelli, F.A. Guardiola, D. Ceballos-Francisco, J. M. García Beltrán, A. Ieni, M.Á. Esteban, Implication of mucus-secreting cells, acidophilic granulocytes and monocytes/macrophages in the resolution of skin inflammation caused by subcutaneous injection of λ/κ-carrageenin to gilthead seabream (*Sparus aurata*) specimens, J. Fish. Dis. (2021) 1–15, https://doi.org/10.1111/jfd.13528, 00.
[41] S.D. Parlee, S.I. Lentz, H. Mori, O.A. MacDougald, Quantifying Size and Number of Adipocytes in Adipose Tissue, first ed., Elsevier Inc., 2014 https://doi.org/10.1016/B978-0-12-411619-1.00006-9.
[42] P. Bankhead, M.B. Loughrey, J.A. Fernández, Y. Dombrowski, D.G. McArt, P. D. Dunne, S. McQuaid, R.T. Gray, L.J. Murray, H.G. Coleman, J.A. James, M. Salto-Tellez, P.W. Hamilton, QuPath, Open source software for digital pathology image analysis, Sci. Rep. 7 (2017) 1–7, https://doi.org/10.1038/s41598-017-17204-5.
[43] J. Folch, M. Lee, G. Stanley, A simple method for the isolation and purification of total lipides from animal tissues, J. Biol. Chem. 226 (1957) 497–509, https://doi.org/10.1016/s0021-9258(18)64849-5.
[44] W. Christie, Lipid Analysis, third ed., The Oily Press, Bridgewater, UK., 2003.

[45] C.S. Pareek, R. Smoczynski, A. Tretyn, Sequencing technologies and genome sequencing, J. Appl. Genet. 52 (2011) 413–435, https://doi.org/10.1007/s13353-011-0057-x.
[46] P. Chomczynski, A reagent for the single-step simultaneous isolation of RNA, DNA and proteins from cell and tissue samples, Biotechniques 15 (1993) 532–537.
[47] K.J. Livak, T.D. Schmittgen, Analysis of relative gene expression data using real-time quantitative PCR and the 2-ΔΔCT method, Methods 25 (2001) 402–408, https://doi.org/10.1006/meth.2001.1262.
[48] H. Cordero, M.F. Brinchmann, A. Cuesta, J. Meseguer, M.A. Esteban, Skin mucus proteome map of European sea bass (*Dicentrarchus labrax*), Proteomics 15 (2015) 4007–4020, https://doi.org/10.1002/pmic.201500120.
[49] M. Bou, X. Wang, M. Todorčević, T.K.K. Østbye, J. Torgersen, B. Ruyter, Lipid deposition and mobilisation in Atlantic salmon adipocytes, Int. J. Mol. Sci. 21 (2020), https://doi.org/10.3390/ijms21072332.
[50] D.B. Hausman, M. DiGirolamo, T.J. Bartness, G.J. Hausman, R.J. Martin, The biology of white adipocyte proliferation, Obes. Rev. 2 (2001) 239–254, https://doi.org/10.1046/j.1467-789X.2001.00042.x.
[51] E.D. Rosen, O.A. MacDougald, Adipocyte differentiation from the inside out, Nat. Rev. Mol. Cell Biol. 7 (2006) 885–896, https://doi.org/10.1038/nrm2066.
[52] A. Albalat, J. Gutiérrez, I. Navarro, Regulation of lipolysis in isolated adipocytes of rainbow trout (*Oncorhynchus mykiss*): the role of insulin and glucagon, Comp. Biochem. Physiol. Mol. Integr. Physiol. 142 (2005) 347–354, https://doi.org/10.1016/j.cbpa.2005.08.006.
[53] L. Cruz-Garcia, A. Saera-Vila, I. Navarro, J. Calduch-Giner, J. Pérez-Sánchez, Targets for TNFα-induced lipolysis in gilthead sea bream (*Sparus aurata* L.) adipocytes isolated from lean and fat juvenile fish, J. Exp. Biol. 212 (2009) 2254–2260, https://doi.org/10.1242/jeb.029025.
[54] M. Todorčević, A. Vegusdal, T. Gjøen, H. Sundvold, B.E. Torstensen, M.A. Kjær, B. Ruyter, Changes in fatty acids metabolism during differentiation of Atlantic salmon preadipocytes; Effects of n-3 and n-9 fatty acids, Biochim. Biophys. Acta, Mol. Cell Biol. Lipids 1781 (2008) 326–335, https://doi.org/10.1016/j.bbalip.2008.04.014.
[55] M. Bou, J. Montfort, A. Le Cam, C. Rallière, V. Lebret, J.C. Gabillard, C. Weil, J. Gutiérrez, P.Y. Rescan, E. Capilla, I. Navarro, Gene expression profile during proliferation and differentiation of rainbow trout adipocyte precursor cells, BMC Genom. 18 (2017) 1–20, https://doi.org/10.1186/s12864-017-3728-0.
[56] C.P. Sewter, J.E. Digby, F. Blows, J. Prins, S. O'Rahilly, Regulation of tumour necrosis factor-alpha release from human adipose tissue *in vitro*, J. Endocrinol. 163 (1999) 33–38, https://doi.org/10.1677/joe.0.1630033.
[57] V.-I. Alexaki, G. Notas, V. Pelekanou, M. Kampa, M. Valkanou, P. Theodoropoulos, E.N. Stathopoulos, A. Tsapis, E. Castanas, Adipocytes as immune cells: differential expression of TWEAK, BAFF, and APRIL and their receptors (Fn14, BAFF-R, TACI, and BCMA) at different stages of normal and pathological adipose tissue development, J. Immunol. 183 (2009) 5948–5956, https://doi.org/10.4049/jimmunol.0901186.
[58] D. Frasca, A. Diaz, M. Romero, S. Thaller, B.B. Blomberg, Secretion of autoimmune antibodies in the human subcutaneous adipose tissue, PLoS One 13 (2018) 1–23, https://doi.org/10.1371/journal.pone.0197472.
[59] J. Pietsch, A. Batra, T. Stroh, I. Fedke, R. Glauben, B. Okur, M. Zeitz, B. Siegmund, Toll-like receptor expression and response to specific stimulation in adipocytes and preadipocytes: on the role of fat in inflammation, Ann. N. Y. Acad. Sci. 1072 (2006) 407–409, https://doi.org/10.1196/annals.1326.021.
[60] A. Kopp, C. Buechler, M. Neumeier, J. Weigert, C. Aslanidis, J. Schölmerich, A. Schäffler, Innate immunity and adipocyte function: ligand-specific activation of multiple toll-like receptors modulates cytokine, adipokine, and chemokine secretion in adipocytes, Obesity 17 (2009) 648–656, https://doi.org/10.1038/oby.2008.607.
[61] Y. Lin, H. Lee, A.H. Berg, M.P. Lisanti, L. Shapiro, P.E. Scherer, The lipopolysaccharide-activated Toll-like receptor (TLR)-4 induces synthesis of the closely related receptor TLR-2 in adipocytes, J. Biol. Chem. 275 (2000) 24255–24263, https://doi.org/10.1074/jbc.M002137200.
[62] J.Y. Huh, J.I. Kim, Y.J. Park, I.J. Hwang, Y.S. Lee, J.H. Sohn, S.K. Lee, A.A. Alfadda, S.S. Kim, S.H. Choi, D.-S. Lee, S.-H. Park, R.H. Seong, C.S. Choi, J.B. Kim, A novel function of adipocytes in lipid antigen presentation to iNKT cells, Mol. Cell Biol. 33 (2013) 328–339, https://doi.org/10.1128/mcb.00552-12.
[63] M. Poggi, J. Jager, O. Paulmyer-Lacroix, F. Peiretti, T. Gremeaux, M. Verdier, M. Grino, A. Stepanian, S. Msika, R. Burcelin, D. De Prost, J.F. Tanti, M.C. Alessi, The inflammatory receptor CD40 is expressed on human adipocytes: contribution to crosstalk between lymphocytes and adipocytes, Diabetologia 52 (2009) 1152–1163, https://doi.org/10.1007/s00125-009-1267-1.
[64] L. Xiao, X. Yang, Y. Lin, S. Li, J. Jiang, S. Qian, Q. Tang, R. He, X. Li, Large Adipocytes Function as Antigen-Presenting Cells to Activate CD4 + T Cells via Upregulating MHCII in Obesity, 2016, https://doi.org/10.1038/ijo.2015.145.
[65] S.P. Weisberg, D. McCann, M. Desai, M. Rosenbaum, R.L. Leibel, A.W. Ferrante, Obesity is associated with macrophage accumulation in adipose tissue, J. Clin. Invest. 112 (2003) 1796–1808, https://doi.org/10.1172/JCI200319246.
[66] K.E. Wellen, G.S. Hotamisligil, Obesity-induced inflammatory changes in adipose tissue, J. Clin. Invest. 112 (2003) 1785–1788, https://doi.org/10.1172/JCI20514.
[67] G. Ravaut, A. Légiot, K.F. Bergeron, C. Mounier, Monounsaturated fatty acids in obesity-related inflammation, Int. J. Mol. Sci. 22 (2021) 1–22, https://doi.org/10.3390/ijms22010330.
[68] C.Y. Tan, A. Vidal-Puig, Adipose tissue expandability: the metabolic problems of obesity may arise from the inability to become more obese, Biochem. Soc. Trans. 36 (2008) 935–940, https://doi.org/10.1042/BST0360935.
[69] K. Frayn, Adipose tissue as a buffer for daily lipid flux, Diabetologia 45 (2002) 1201–1210, https://doi.org/10.1007/s00125-002-0873-y.
[70] L.D. Ly, S. Xu, S.-K. Choi, C.-M. Ha, T. Thoudam, S.-K. Cha, A. Wiederkehr, C. B. Wollheim, I.-K. Lee, K.-S. Park, Oxidative stress and calcium dysregulation by palmitate in type 2 diabetes, Exp. Mol. Med. 49 (2017), https://doi.org/10.1038/emm.2016.157 e291–e291.
[71] J.Y. Lee, K.H. Sohn, S.H. Rhee, D. Hwang, Saturated fatty acids, but not unsaturated fatty acids, induce the expression of cyclooxygenase-2 mediated through Toll-like receptor 4, J. Biol. Chem. 276 (2001) 16683–16689, https://doi.org/10.1074/jbc.M011695200.
[72] M.P. Sepulcre, F. Alcaraz-Pérez, A. López-Muñoz, F.J. Roca, J. Meseguer, M. L. Cayuela, V. Mulero, Evolution of lipopolysaccharide (LPS) recognition and signaling: fish TLR4 does not recognize LPS and negatively regulates NF-κB activation, J. Immunol. 182 (2009) 1836–1845, https://doi.org/10.4049/jimmunol.0801755.
[73] I. Popa, The concept of sphingolipid rheostat in skin: a driving force for new active ingredients in cosmetic applications, OCL - oilseeds Fats, Crop. Lipids. 25 (2018), https://doi.org/10.1051/ocl/2018043.
[74] N. Makdissy, K. Haddad, C. Mouawad, I. Popa, M. Younsi, P. Valet, L. Brunaud, O. Ziegler, D. Quilliot, Regulation of SREBPs by sphingomyelin in adipocytes via a caveolin and Ras-ERK-MAPK-CREB signaling pathway, PLoS One 10 (2015) 1–33, https://doi.org/10.1371/journal.pone.0133181.
[75] W.S. Powell, J. Rokach, Biosynthesis, biological effects, and receptors of hydroxyeicosatetraenoic acids (HETEs) and oxoeicosatetraenoic acids (oxo-ETEs) derived from arachidonic acid, Biochim. Biophys. Acta, Mol. Cell Biol. Lipids 1851 (2015) 340–355, https://doi.org/10.1016/j.bbalip.2014.10.008.